Cellular Microbiology (2011) doi:10.1111/j.1462-5822.2011.01610.x

The FbaB-type fibronectin-binding protein of *Streptococcus pyogenes* promotes specific invasion into endothelial cells

Silva Amelung,[1] Andreas Nerlich,[1] Manfred Rohde,[1] Barbara Spellerberg,[2] Jason N. Cole,[3†] Victor Nizet,[3] Gursharan S. Chhatwal[1] and Susanne R. Talay[1*]

[1]*Department of Medical Microbiology, Helmholtz Centre for Infection Research, 38124 Braunschweig, Germany.*

[2]*Department of Medical Microbiology and Hygiene, University Hospital Ulm, Ulm, Germany.*

[3]*Department of Pediatrics and Skaggs School of Pharmacy & Pharmaceutical Sciences University of California, San Diego, La Jolla, CA 92093, USA.*

Summary

Invasive serotype M3 *Streptococcus pyogenes* are among the most frequently isolated organisms from patients suffering from invasive streptococcal disease and have the potential to invade primary human endothelial cells (EC) via a rapid and efficient mechanism. FbaB protein, the fibronectin-binding protein expressed by M3 *S. pyogenes*, was herein identified as a potent invasin for EC. By combining heterologous gene expression with allelic replacement, we demonstrate that FbaB is essential and sufficient to trigger EC invasion via a Rac1-dependent phagocytosis-like uptake. FbaB-mediated uptake follows the classical endocytic pathway with lysosomal destination. FbaB is demonstrated to be a streptococcal invasin exhibiting EC tropism. FbaB thus initiates a process that may contribute to the deep tissue tropism and spread of invasive *S. pyogenes* isolates into the vascular EC lining.

Introduction

Streptococcus pyogenes (group A *Streptococcus*, GAS) is an important human pathogen that causes superficial infections of the pharyngeal mucosa and the skin (Cunningham, 2000). GAS can also produce severe invasive deep tissue infections such as necrotizing fasciitis, which are frequently complicated by toxic shock-like syndrome (TSLS) (Stevens, 2000). Streptococcal TSLS is a life-threatening condition associated with high mortality rates despite intensive medical treatment. In the last few decades, research has focused on the identification of GAS toxins and immune evasion factors involved in the pathogenesis of invasive disease. Less attention has been focused on the diversity and specificity of GAS adhesins and invasins, and how these molecules govern cell and tissue tropism to impact the spectrum of diseases that a particular strain can cause.

Fibronectin-binding proteins have been identified as potent adhesins in a variety of pathogenic Gram-positive cocci (Talay, 2005; Schwarz-Linek *et al*., 2006). The high-affinity binding of this class of covalently linked surface molecules to fibronectin forms the structural basis for their unique biological function (Schwarz-Linek *et al*., 2003). Epithelial cell adhesion and invasion may be responsible for the localized tissue tropism of the pathogen to the oropharynx. M3 GAS do not possess the genes for SfbI/PrtF1, or M1, two major epithelial cell adhesins and invasins of GAS. However, epidemiological studies revealed that GAS strains harbouring the *prtF2* gene, which encodes the fibronectin-binding protein F2/PFBP (Jaffe *et al*., 1996; Rocha and Fischetti, 1999), are associated with invasive infections (Delvecchio *et al*., 2002). Within this gene family, two mutually exclusive genotypes exist, the *pfbp* type and the *fbaB* type (Ramachandran *et al*., 2004). The *fbaB* gene is highly conserved and located within the fibronectin-collagen-T antigen (FCT) region of GAS, a locus harbouring genes coding for adhesins that interact with extracellular matrix molecules and for pilus-forming proteins (Bessen and Kalia, 2002; Mora *et al*., 2005; Telford *et al*., 2006). The *fbaB* gene was first discovered in an M3 GAS strain isolated from a TSLS patient and is predominantly expressed by M3 strains isolated from patients suffering from invasive GAS disease (Terao *et al*., 2002).

Serotype M3 GAS have been isolated worldwide from patients with invasive GAS disease (Stevens *et al*., 1989; Inagaki *et al*., 2000). How M3 GAS spread from the pharyngeal mucosal surface into deep tissue is unknown. A

Received 6 January, 2011; revised 24 March, 2011; accepted 5 April, 2011. *For correspondence. E-mail: susanne.talay@helmholtz-hzi.de; Tel. (+49) 531 6181 4413; Fax (+49) 531 6181 4499.
†Present address: School of Chemistry and Molecular Biosciences, The University of Queensland, Brisbane, St Lucia, Qld 4072, Australia.

hallmark of deep tissue infection and/or systemic spread of a pathogen is its ability to cross cellular and tissue barriers, leading to the concept that invasive GAS spread into deep tissue as a complication of transient bacteraemia (Stevens, 2000). We recently reported that M3 GAS efficiently invades human primary endothelial cells (EC), a process that may represent a prerequisite for *trans*-cellular passage across the endothelial barrier (Nerlich *et al*., 2009). Here, we identify FbaB as potent EC invasin of M3 GAS that is necessary and sufficient to trigger a rapid phagocytosis-like uptake of streptococci into ECs. FbaB triggers uptake via Rac1 recruitment and activation and follows the endocytic pathway with lysosomal destination. FbaB is the first streptococcal factor identified to mediate vascular cell tropism.

Results

FbaB is a potent invasin for EC

An EC non-invasive strain of *Streptococcus agalactiae* (GBS) was used as model organism for heterologous expression of FbaB to study the protein's role during EC infection by gain-of-function analysis. The intact full-length GAS *fbaB* gene was cloned into the *Escherichia coli–Streptococcus* shuttle vector pDCerm generating p*fbaB*, which was then used for heterologous expression of FbaB on the surface of GBS. Using an FbaB-specific antiserum FbaB expression was visualized on the surface of an invasive M3 GAS isolate (Fig. 1A) as well as on the surface of the heterologous GBS strain (Fig. 1B). FbaB-expressing GBS were analysed in an *in vitro* EC invasion assay using primary human EC. As shown in Fig. 1C, FbaB expressing GBS exhibited a strong invasion potential on EC, yielding 21 [mean ± 11.2 standard deviation (SD)] intracellular streptococci per cell after 2 h of infection, whereas the GBS WT strain was not invasive with less than 3 bacteria per 100 cells (mean ± 0.032 SD, Fig. 1D). The parental M3 GAS revealed 7.3 (mean ± 1.9 SD) intracellular bacteria per cell after 2 h of infection. Electron microscopic images of infected EC also revealed the presence of extracellular and intracellular streptococci on and within EC (Fig. 1E–G). To prove that GAS FbaB is sufficient to promote EC cell entry, an inert latex bead EC internalization assay (Kaur *et al*., 2010) was undertaken. Beads coated with GST-FbaB protein were efficiently internalized by EC (Fig. 1H–J), but not control beads coated with GST. Together, our results demonstrate that FbaB is sufficient to confer efficient uptake of bacteria and inert particles into EC.

FbaB triggers a phagocytosis-like uptake with lysosomal destination

FbaB belongs to a family of fibronectin-binding proteins harbouring several C-terminal repeats that form high-affinity complexes with fibronectin (Schwarz-Linek *et al*., 2003). SfbI protein, another member of this protein family, acts as epithelial cell invasin by triggering caveolae-mediated, non-phagocytic uptake of *S. pyogenes* (Rohde *et al*., 2003) resulting in a persistent non-lysosomal intracellular stage. In contrast to this, serotype M3 *S. pyogenes* invade EC via the zipper mechanism, accompanied by localized F-actin accumulation, as well as Rac1 accumulation and activation (Nerlich *et al*., 2009) and are delivered into lysosomes (S.R. Talay, unpublished). It was thus of interest to determine the mode of uptake and subsequent trafficking within EC that was promoted by FbaB. FbaB-mediated uptake of bacteria and latex beads resembles phagocytic uptake via a zipper mechanism (Fig. 2A and B). The molecular basis for the formation of the membrane protrusions on the EC membrane is a massive but short-lived F-actin accumulation at the entry port (Fig. 2C).

Fig. 1. FbaB mediates invasion into ECs.
A. FbaB surface expression of WT M3 GAS. Immunofluorescent (IF)-labelled FbaB (green) on M3 GAS (blue) and FESEM (insert) image of immunolabelled FbaB on M3 GAS.
B. Heterologous expression of FbaB on the surface of *S. agalactiae* (GBS). IF image of immunolabelled FbaB (green) on the surface of the heterologous FbaB-expressing GBS strain (blue), and lack of FbaB expression on WT GBS (insert).
C. Invasive potential of GBS-FbaB on EC. HUVEC were infected with GBS-FbaB for 2 h, washed fixed and differentially stained for extra- and intracellular streptococci. IF image of a cell infected with GBS-FbaB; intracellular cocci are red, extracellular green. Figure S1A shows phase contrast of the same field.
D. Quantification of EC invasion. Invasion rates were determined by enumerating intracellular (red) bacteria and expressed as intracellular bacteria per 10 cells. The diagram shows invasion rates of GBS-FbaB, the GBS-WT strain and the parental M3 GAS isolate A60 after 2 h of infection (***$P < 0.0001$).
E. FESEM image of adherent and intracellular FbaB-expressing GBS after 2 h of infection.
F and G. TEM image of ultrathin sections of GBS-FbaB infected EC after 2 h of infection.
H. Uptake of FbaB-coated polystyrene beads into EC. IF image of extracellular (yellow) and intracellular (red) FbaB-coated beads on one EC after 2 h of co-incubation. Figure S1B shows phase contrast of the same field.
I. FESEM image of one adherent and one internalized FbaB-coated bead on EC.
J. Quantification of bead internalization into HUVEC. Internalization rates were determined after 1 h co-incubation by enumerating intracellular (red) beads. '100% Intracellular beads' refers to a mean of 5.5 FbaB-coated beads per cell (SD ± 0.4). Control beads were coated with GST, revealing a mean of 0.35 intracellular beads per cell (SD ± 0.3; ***$P < 0.0002$).
Bars represent 1 μm (H), 5 μm (A, B, C, E, G), 2 μm (F, I) or 0.5 μm (A, insert).

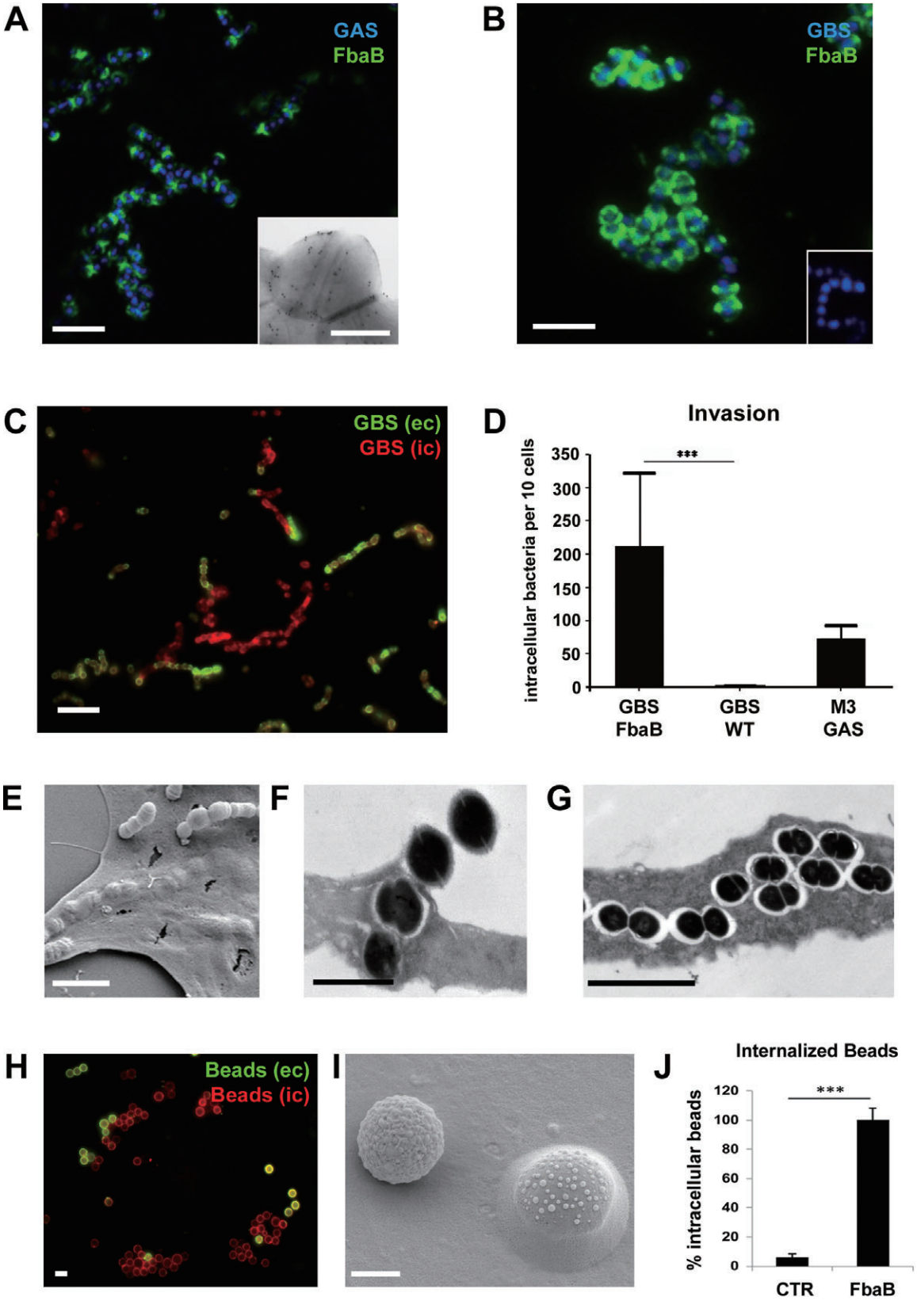

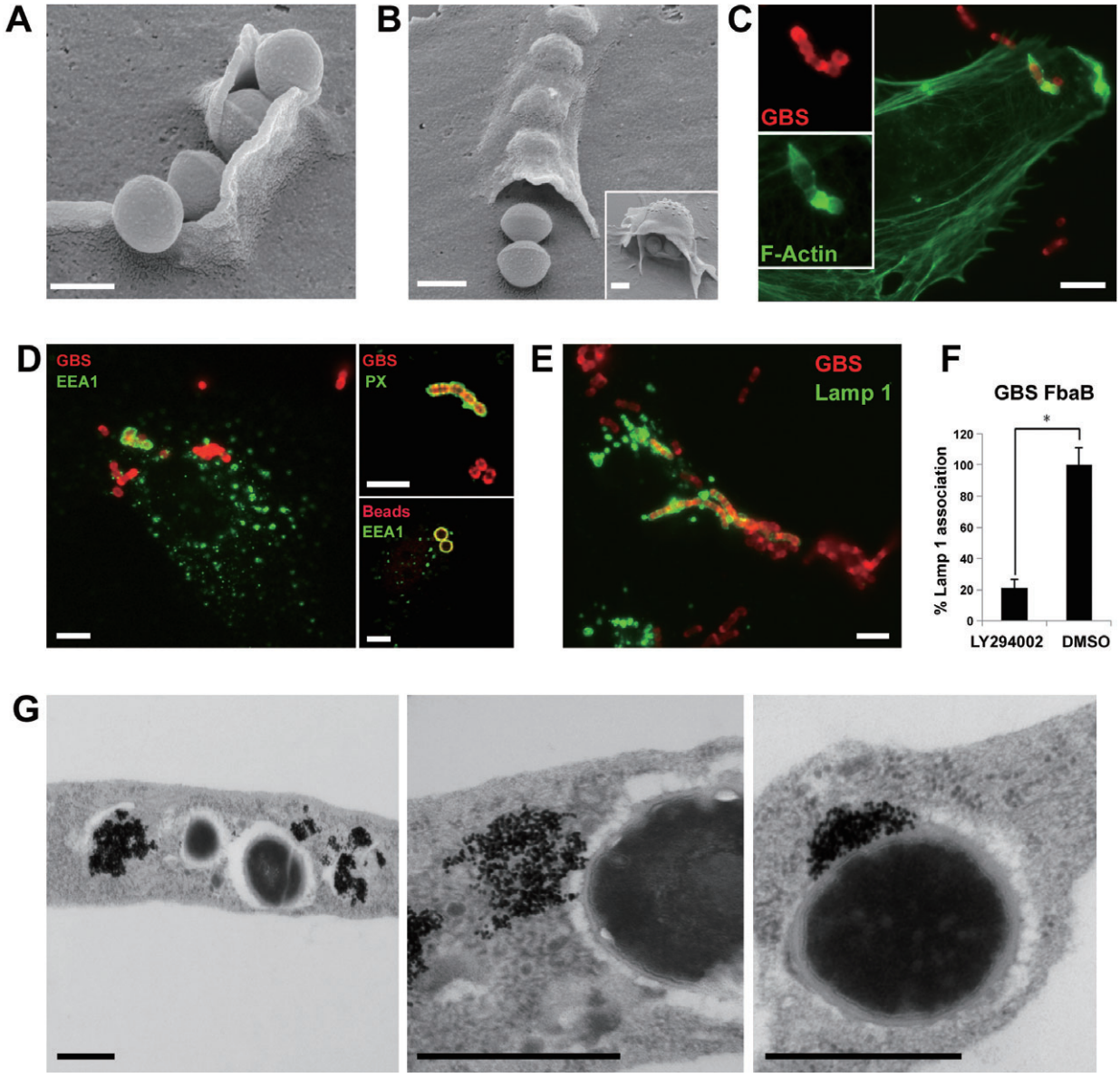

Fig. 2. FbaB triggers phagocytosis-like uptake in EC with lysosomal destination.
A. Phagocytosis-like uptake of FbaB-expressing GBS into EC. Membrane protrusions along an adherent streptococcal strain characterize the initial uptake process after 30 min of infection.
B. Closure of the EC membrane leads to streptococcal internalization. The insert demonstrates formation of equal structures on EC upon internalization of FbaB-coated beads.
C. IF image showing F-actin (green) accumulation at the entry site of streptococci (red); the inserts show split channels for F-actin and GBS at higher magnification.
D–F. FbaB-mediated uptake follows the classical endocytic pathway.
D. IF image of FbaB-GBS (red) that accumulate the early endosomal marker protein EEA1 (green) after EC entry (60 min post infection). The upper insert shows accumulation of the DsRed-labelled PX domain of $p40^{Phox}$ (DsRed-PX, pseudo-coloured in green) around an internalized streptococcal chain (pseudo-coloured in red), the lower insert shows circumferential accumulation of EEA1 (green) on an internalized FbaB-coated bead (red).
E. IF image of FbaB-GBS (red) that accumulate the late endosomal/lysosomal marker protein Lamp-1 (green) during the progress of infection (120 min post infection).
F. Quantification of inhibition of lysosomal fusion after 2 h of infection using the PI3 kinase (PI3K)-specific inhibitor LY294002. '100% Lamp 1 association' refers to a mean of 22.7 Lamp-1 associated cocci per cell (SD ± 2.4; $^{***}P < 0.002$).
G. TEM image of ultrathin sections of GBS-FbaB infected EC. Different stages of the fusion events of GBS-FbaB with BSA-gold-loaded terminal lysosomes are shown. The right image shows gold particles in close association with a bacterial cell, indicating successful fusion of the phagosome with a terminal lysosome.
Bars indicate 1 μm (A, B, G) and 5 μm (C, D, E).

We next assessed whether this zipper-like uptake leads into the classical endocytic pathway. GBS-FbaB accumulate the early endosomal marker protein EEA1 around invading bacterial chains, suggesting early endosomal localization (Fig. 2D). This finding was further corroborated by transfecting EC with the DsRed/TagRFP-labelled PX domain of $p40^{PHOX}$, which binds to phosphatidylinositol-3-phosphate (PtdIns(3)P) generated by class III PI3K on the membranes of early endosomes (Ellson *et al*., 2001). Recognition of membrane incorporated PtdIns(3)P by FYVE and PX domain-containing sorting proteins is an essential event for endosomal fusion and subsequent vesicular trafficking into lysosomes (Vieira *et al*., 2001). Infection of PX-DsRed/TagRFP-expressing cells demonstrated circumferential accumulation of the PX domain on intracellular streptococcal chains (upper insert in Fig. 2D). FbaB-coated latex beads also followed the endocytic pathway and colocalized with EEA1 (lower insert in Fig. 2D) as well as the PX domain (not shown). Since the GBS WT strain was not invasive in HUVEC, there was also no colocalization with intracellular marker proteins such as F-actin, EEA-1 and PX-domain (data not shown).

The later stages of intracellular trafficking were determined by testing for the acquisition of late endosomal/lysosomal marker protein Lamp-1 in the phagosomal membrane. Lamp-1 accumulated around intracellular FbaB-expressing GBS after 2 h of infection, indicating streptococcal trafficking into the late endosomal/lysosomal compartment (Fig. 2E). Inhibition of lysosomal fusion with LY294002, a PI3 kinase (PI3K)-specific inhibitor, substantially reduced the number of Lamp-1-associated streptococci (Fig. 2F) revealing that streptococcal entry follows the endocytic pathway. To finally assess whether FbaB-mediated uptake leads to fusion of streptococci-containing phagosomes with terminal lysosomes, the latter were pre-loaded with BSA-gold particles. Close association of gold particles with FbaB-expressing GBS (Fig. 2G) demonstrates that bacteria fuse with terminal lysosomes. The WT GBS strain did not colocalize with Lamp-1 or BSA-gold particles since it was not invasive in HUVEC (data not shown). These data provide evidence that FbaB triggers phagocytic uptake of the bacteria, and engages the classical endocytic pathway for subsequent trafficking of bacteria into terminal lysosomes.

The small GTPase Rac1 is an essential host factor for FbaB-mediated invasion

A rapid phagocytosis-like uptake requires whole-scale cytoskeletal rearrangements that are operated by the family of small GTPases. We therefore assessed the role of Rac1 in the FbaB-mediated entry process. Transfection of EC with EGFP-fused WT Rac1 and subsequent infection with GBS-FbaB revealed longitudinal accumulation of Rac1 along an invading chain (Fig. 3A and Movie S1). These changes are paralleled by simultaneous F-actin accumulation (Fig. 3B). Expression of the dominant negative form of Rac1 (N17) significantly reduced the number of intracellular bacteria, whereas expression of WT Rac1 significantly enhanced uptake of FbaB-expressing GBS in comparison with EGFP-expressing cells (Fig. 3C), clearly demonstrating that Rac1 is an essential factor for FbaB-mediated uptake. To analyse the activation of Rac1 we used a fluorescently tagged Cdc42 and Rac1 interactive binding domain (CRIB) fused to TagRFP (CRIB-TagRFP) as a biosensor of Rac activation (Itoh *et al*., 2002). Infection of transiently transfected cells results in accumulation of CRIB-TagRFP at the site of GBS-FbaB entry (Fig. 3D) as well as accumulation of the CRIB-TagRFP at the site of M3 GAS entry (Fig. 3E). These data indicate that FbaB triggers Rac1 recruitment and activation during the process of entry.

FbaB is an invasin with EC tropism

Our gain-of-function analysis demonstrated the potential for FbaB to function as a potent invasin for primary human EC. We finally aimed to find out, whether FbaB exhibited a higher affinity to human EC compared with epithelial cells. To assess this, we conducted a mixed cell infection experiment, in which epithelial and endothelial cells were infected simultaneously in the same well. FbaB-expressing GBS as well as M3 GAS exhibited a strong preference for EC compared with epithelial cells (HEp-2) of human origin (Fig. 4). In the same set of experiments, HEp-2 cells were also infected with a serotype M12 strain expressing the epithelial cell invasin SfbI as positive control (Rohde *et al*., 2011). Figure S2E shows quantification of the invasion potential of the HEp-2 invasive M12 GAS isolate in comparison with the M3 GAS strain A60 as well as the FbaB-expressing GBS strain. The invasion potential of the SfbI protein-expressing M12 strain was more than 20-fold enhanced compared with the M3 GAS strain and more than 10-fold enhanced compared with the FbaB-expressing GBS strain. This underlines that in contrast to SfbI protein, FbaB is a poor invasin on HEp-2 cells. In a final set of experiments we constructed a loss of function mutant in the M3 GAS background by allelic replacement and determined the invasion potential of the FbaB mutant GAS strain (Fig. 5). In the FbaB mutant strain, a more than 70% reduction of the EC invasion potential was observed. As a control, the fibronectin-binding activity of the mutant strain was also monitored and revealed loss of fibronectin-binding activity. These data show that in our representative M3 GAS strain, FbaB is the only fibronectin-binding factor and an essential factor for EC tropism and invasion.

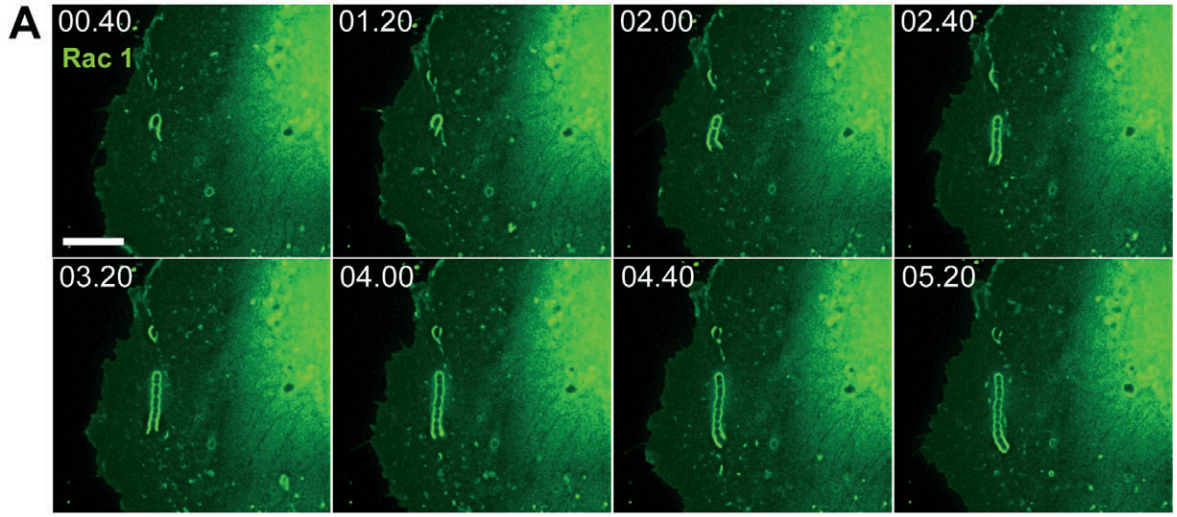

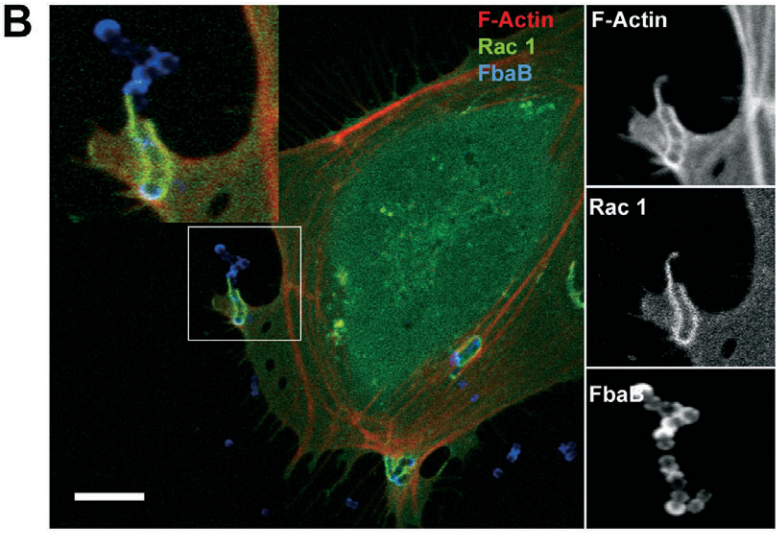

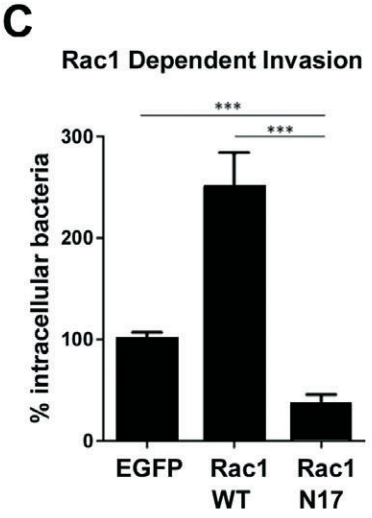

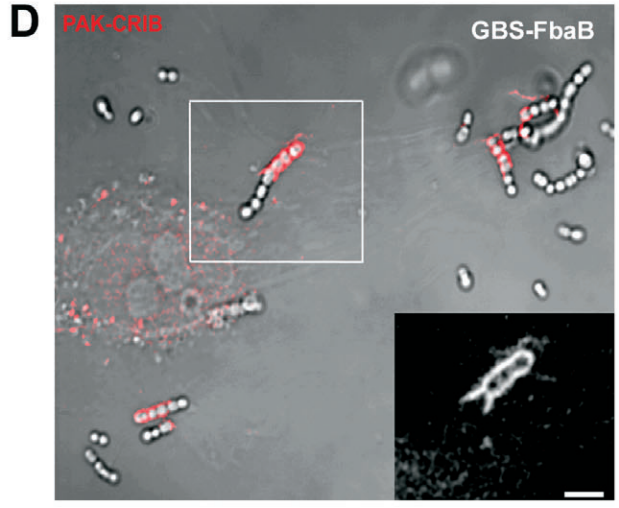

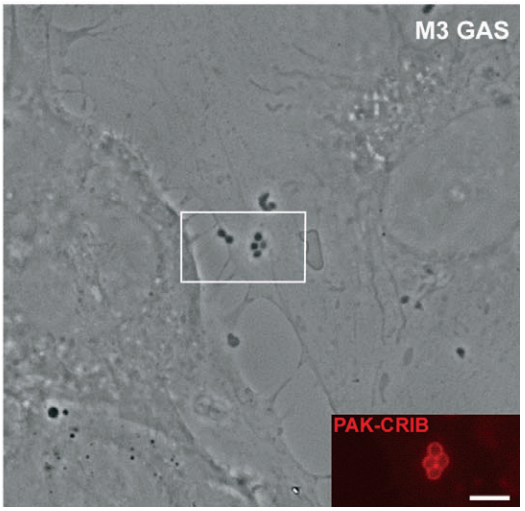

Fig. 3. Essential role of the small GTPase Rac1 in the FbaB-mediated EC invasion process.
A. Time-lapse microscopy of GBS-FbaB entry into EGFP-WT Rac1-transfected EC. Eight frames of Movie S1 show subsequent accumulation of Rac1 along a streptococcal chain during the first minutes of invasion.
B. IF image of GFP-Rac1-expressing EC infected with GBS-FbaB for 60 min (red: F-actin, green: Rac1, blue: FbaB). Inserts at the right side show split channels for F-actin, Rac1 and FbaB stain (from up to down).
C. Quantification of FbaB-mediated invasion into EC that express either wild-type Rac1 (WT Rac1), the dominant-negative form of Rac1 (Rac-N17) or EGFP (EGFP) demonstrates that Rac1 is essential for invasion. Invasion rates were determined by enumerating intracellular (red) bacteria after 2 h of infection. EGFP-transfected cells served as control with '100% invasion' referring to 24 intracellular cocci per cell (***$P < 0.0001$).
D. Phase-contrast/fluorescence image of infected EC expressing the PAK-CRIB domain as RFP-fusion protein (CRIB-TagRFP). GBS-FbaB-induced Rac1 activation was visualized by demonstrating accumulation of the PAK-CRIB domain (red) along an invading streptococcal chain after 60 min of infection. The insert shows an enlargement of the fluorescence channel of the indicated area.
E. Phase-contrast/fluorescence image of M3 GAS-infected EC expressing the PAK-CRIB domain. The insert shows an enlargement of the fluorescence channel of the indicated area.
Bars represent 10 μm (A, B) or 3 μm (D, E).

Discussion

Invasive M3 streptococci have a strong potential to invade primary human EC (Nerlich *et al.*, 2009), a feature that likely represents an important step towards crossing the endothelial barrier during dissemination to the tissues. M3 GAS do not possess the gene for SfbI/PrtF1, an important invasin of GAS, but instead carry the *fbaB* gene within the FCT region. We here identified FbaB as the major EC invasin of M3 GAS, and demonstrate that FbaB is necessary and sufficient to mediate this function. Phagocytosis is a process by which particles or live bacteria are taken

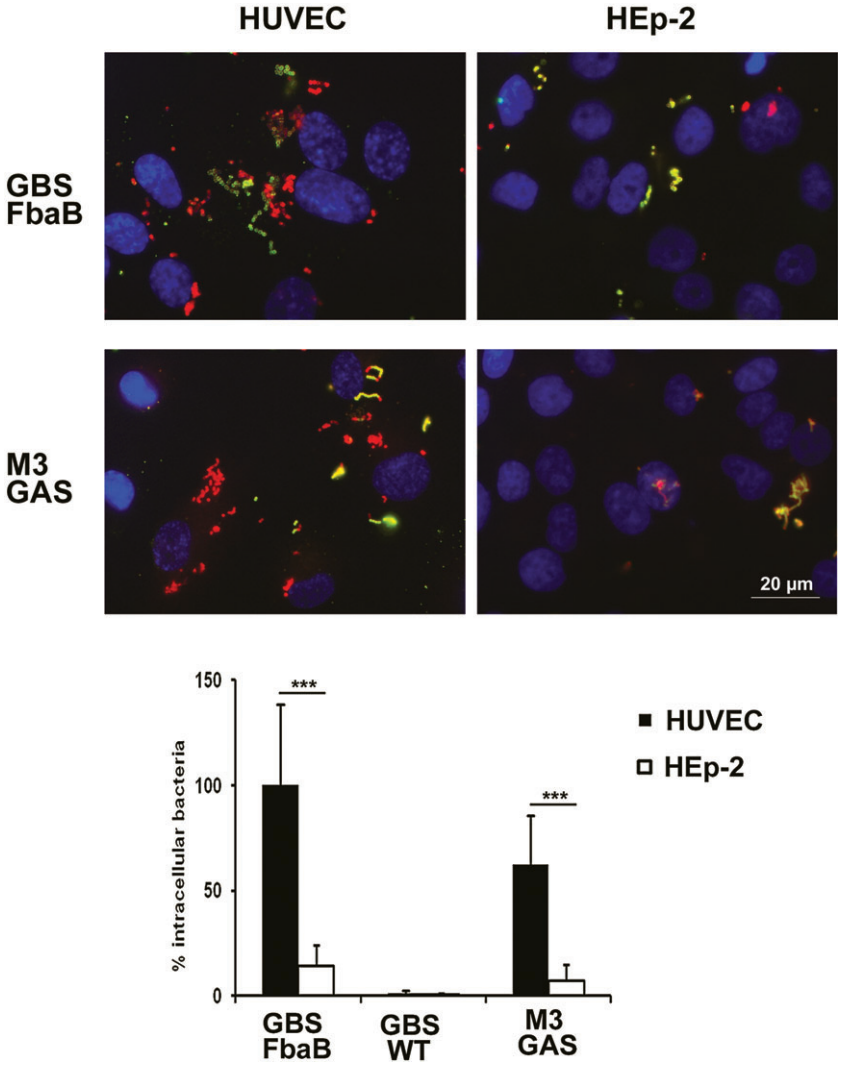

Fig. 4. FbaB is an invasin with endothelial cell tropism. HUVEC and HEp-2 cell (human epithelial cell line) were seeded on coverslips, placed into the same well and grown to confluency in EGM2 medium. Cells were infected for 2 h with an moi of 25 with GBS WT or GBS-FbaB, or an moi of 50 with M3 GAS bacteria. Intracellular bacteria were stained in red, extracellular in green.
A. IF image of FbaB-expressing GAS and GBS strains infecting HUVEC (left panel) or Hep-2 cells (right panel). Phase-contrast images are shown in Fig. S2A–D.
B. Invasion rates were determined by counting intracellular (red) bacteria per cell. '100% invasion' refers to 19 intracellular bacteria per cell [mean of four independent experiments (SD ± 7.3; ***$P < 0.0001$)].

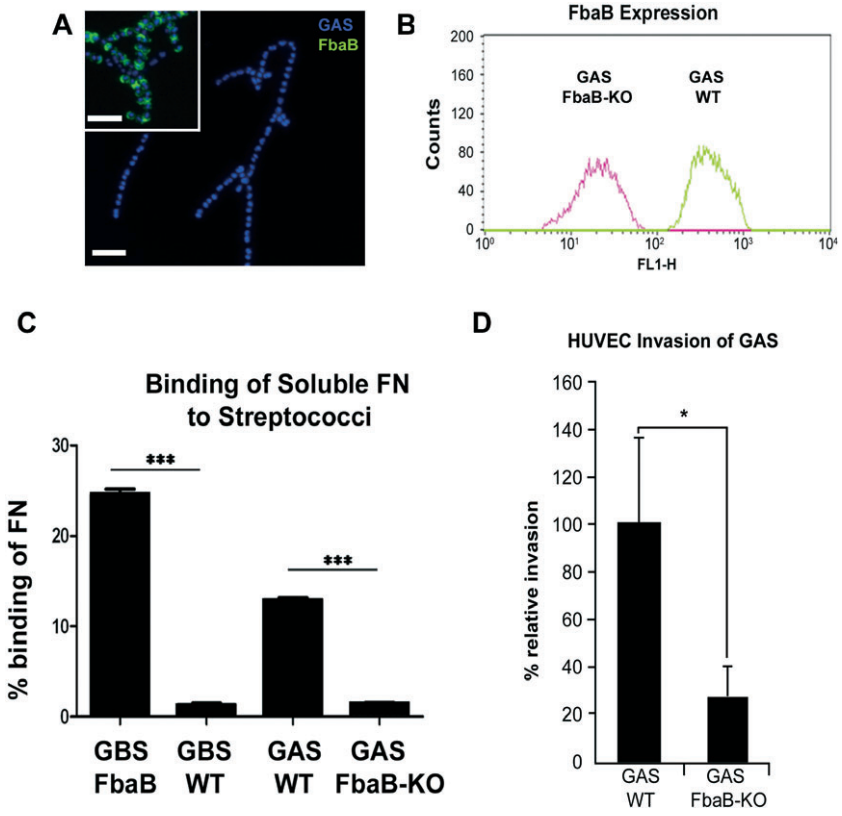

Fig. 5. FbaB is the major EC invasin of M3 *S. pyogenes*.
A. Generation of a loss of function mutant (GAS FbaB-KO) in invasive M3 GAS and lack of FbaB surface expression in the deletion mutant. IF image of lacking FbaB surface expression (green) in the mutant, FbaB surface expression of WT M3 GAS (insert in A). GAS were visualized with DAPI (blue). Identical settings were used to acquire both images. Bars represent 5 μm.
B. Quantification of FbaB surface expression in the WT M3 GAS strain and the GAS FbaB-KO mutant by flow cytometry analysis. Fluorescence was analysed from 5000 bacteria, using a polyclonal anti-FbaB rabbit antibody in combination with an anti-rabbit Alexa Fluor® 488 secondary antibody.
C. FbaB-dependent 'loss of function' and 'gain of function' of the fibronectin-binding activity on the surface of GAS and GBS. Quantification of fibronectin-binding activity of streptococci either lacking FbaB expression (GBS WT, GAS FbaB-KO) or expressing FbaB (GAS WT, GBS-FbaB) revealed that FbaB is essential but also sufficient to mediate binding of soluble radiolabelled fibronectin in a whole-cell binding assay (***$P < 0.0001$).
D. Quantification of the EC invasion potential of WT GAS in comparison with the GAS FbaB-KO mutant revealed a significant reduction of the invasion potential in the loss of function mutant. Invasion rates were determined after 2 h of infection by counting intracellular (red) bacteria per cell. '100% invasion' refers to 7.4 intracellular bacteria per cell (SD ± 1.9; ***$P < 0.0001$).

up and delivered into terminal lysosomes via the classical endocytic pathway (Haas, 2007). FbaB-mediated entry showed typical features of classical phagocytosis: (i) formation of membrane protrusions and close engulfment of the bacterium at the entry site, (ii) massive F-actin accumulation surrounding invading streptococci with co-incident Rac1 accumulation and activation, (iii) subsequent acquisition of early and late endosomal marker proteins in the phagosomal membrane, and (iv) final delivery into terminal lysosomes. This mechanism bears resemblance to M1 protein-mediated uptake of M1 GAS strains in epithelial cells (Dombek *et al*., 1999), but differs completely from the caveolae-mediated epithelial cell uptake triggered by SfbI (Rohde *et al*., 2003), a structurally related but distinct GAS fibronectin-binding protein. SfbI protein is equally potent to mediate epithelial and endothelial cell invasion *in vitro*. However, since SfbI expression depends on high O_2 and low CO_2 concentration, SfbI will not be expressed under conditions that exist in the bloodstream, resulting in a regulatory tropism for mucosal surfaces rather than deep tissue. This is supported by the finding that the *sfbI* gene is prevalent in strains isolated from patients with persisting asymptomatic GAS carriage (Neeman *et al*., 1998). M3 GAS lack SfbI/PrtF1, a fact that may explain its weak invasive potential on HEp-2 cells. In contrast to this, FbaB is expressed by M3 GAS, and members of the PrtF2 family in general are expressed by strains from invasive disease patients (Delvecchio *et al*., 2002; Terao *et al*., 2002). Here, we identified FbaB as potent EC invasin that can be functionally discriminated from other fibronectin-binding proteins such as SfbI and M1 by its unique ability to trigger

phagocytic uptake into EC. Moreover, in contrast to other invasins from Gram-positive cocci, FbaB shows tropism for EC and thus may be one of the initial factors responsible for the deep tissue tropism of M3 GAS. A further requisite would then be the ability of GAS to leave the EC at the tissue side in a viable form (S.R. Talay, unpublished). The question arises, why FbaB (and also M3 GAS) has a strong preference for EC. Fibronectin is a common ligand for both, SfbI protein and FbaB, and is an essential molecule for SfbI-mediated invasion into epithelial cells (Talay *et al*., 2000). One may thus speculate that FbaB could have a different structural impact on its ligand fibronectin than SfbI protein. This may be due to the lacking element of the UR/Spacer region found in SfbI, or the presence of putative integrin binding sites as well as two CnaB domains, which are important structure-defining elements. Interestingly, the CnaB2 domain of FbaB forms an isopeptide bond that renders the protein highly thermostable and acid resistant (Hagan *et al*., 2010). These additional elements may either constitute or present EC-specific binding sites for receptors that are not found on epithelial cells such HEp-2.

FbaB is the first streptococcal factor identified to mediate EC-specific invasion of GAS and the human endothelium may thus represent a reservoir for serotype M3 and other FbaB-expressing group A streptococci.

Experimental procedures

Bacterial strains and culture conditions

Streptococcus pyogenes strain A60 is a serotype M3 GAS isolated from blood of a patient suffering from invasive disease (Dinkla *et al*., 2003). *S. pyogenes* A40 is an SfbI-expressing epithelial cell invasive M12 GAS and was described previously (Rohde *et al*., 2011). *S. agalactiae* serotype Ia strain 102 was described previously (Kaur *et al*., 2010) and served as the recipient for the plasmid pDCerm (Zinkernagel *et al*., 2008) or the FbaB-expressing plasmid p*fbaB* (this work). Streptococci were cultured in tryptic soy broth (TSB, Oxoid) at 37°C and 5% CO_2, containing 2 μg ml^{-1} erythromycin for selection of plasmid pDCerm and its derivative p*fbaB*; 2 μg ml^{-1} erythromycin and 1 μg ml^{-1} chloramphenicol for selection of pKO-*fbaB* transformants (this work); and 1 μg ml^{-1} chloramphenicol for selection of GAS FbaB-KO. *E. coli* TOP10 (Invitrogen) was grown in Luria–Bertani (LB) broth or on LB plates supplemented with 100 μg ml^{-1} ampicillin, 500 μg ml^{-1} erythromycin or 5 μg ml^{-1} chloramphenicol, where appropriate. To obtain electrocompetent GAS and GBS cells, strains were grown in Todd–Hewitt broth (THB) containing 0.6% glycine. For FACS analysis and infection experiments, GAS and GBS strains were grown to logarithmic phase, corresponding to an OD_{600} of 0.4.

Reagents and antibodies

Rabbit polyclonal antibodies specifically recognizing *S. pyogenes* (anti-GAS) were generated as described previously (Talay *et al*., 2000). Polyclonal anti-GBS antibody was obtained from Acris (Herford, Germany). A mouse monoclonal antibody recognizing a luminal epitope of human Lamp-1 (clone H4A3) was purchased from Pharmingen. Secondary goat anti-rabbit IgG antibodies coupled to ALEXA Fluor® 488/568, and goat anti-mouse IgG coupled to ALEXA Fluor® 488 were obtained from Invitrogen; Cy-5-conjugated goat anti-rabbit IgG was purchased from Millipore (Schwalbach/Ts, Germany). PI3K inhibitor LY294002 was obtained from Calbiochem.

Allelic exchange mutagenesis of GAS

An in-frame allelic exchange of *fbaB* with chloramphenicol acetyltransferase (*cat*) was obtained in *S. pyogenes* A60 by using the method previously described (Zinkernagel *et al*., 2008). The primer pair used for amplification of the upstream fragment flanking the *fbaB* gene was *fbaB*-upF (5′-GCGAATTCGATGG ATTGTTTGTTGGCAAGTC-3′) and *fbaB*-upR (5′-GGTGGT ATATCCAGTGATTTTTTTCTCCATTATTTTCTCTCTCCACATTC CTAAGCG-3′). The primer pair used for amplification of the downstream fragment flanking *fbaB* was *fba*B-downF (5′-TACTGCGATGAGTGGCAGGGCGGGGCGTAACTGTTGGTGA CAATAGCGAAAAAG-3′) and *fbaB*-downR (5′-GCGAATTCAG CTTCGATGCTGTTTAGTTCGTAT-3′). The cat gene was amplified using primers *cat*F (5′-ATGGAGAAAAAAATCACTGGATAT ACCACCGTTGA-3′) and *cat*R (5′-TTACGCCCCGCCCTGC CACTCATCGCAGTACTGTTGTA-3′).

Heterologous expression of FbaB

Streptococcus agalactiae strain 101 was selected as model organism for FbaB expression since this WT GBS strain was tested to be non-invasive in HUVEC yielding less than 3 intracellular bacteria per 100 cells at an moi of 25 (S.R. Talay, unpublished), and previously used to determine whether SpyCep, the IL-8-degrading cell envelope protease of GAS, acts as invasin (Kaur *et al*., 2010). The complete M3 *S. pyogenes fbaB* gene and its flanking regions, starting 68 nucleotides upstream of the start codon and terminating 100 nucleotides downstream of the stop codon, was PCR-amplified from the GAS chromosome, cloned into the TOPO vector (Gateway), and then subcloned into pDCerm (Zinkernagel *et al*., 2008). Primers for amplification were *fbaB*-KpnI-F (5′-GCGGGTACCGACAATTGGCCTGTAGTCTTT AGTTTTGGAC-3′) and *fbaB*-XbaI-R (5′-GCGTCTAGACTTAAAA TGACTTATCTAGTGAACCGAGACG-3′). The resulting plasmid, p*fbaB*, was transformed into electrocompetent *S. agalactiae* cells and transformants (GBS-FbaB) were pre-selected for on erythromycin-containing media and further confirmed by restriction enzyme analysis and PCR. The empty vector was transformed in *S. agalactiae* and the resulting transformant (GBS-pDCerm) used as a negative control. For heterologous expression and subsequent purification of recombinant FbaB protein in *E. coli*, the truncated *fbaB* gene lacking the sequence encoding the signal peptide and membrane anchor was cloned into pGEX-6-P1 (Invitrogen). Primers for amplification were *fbaB*-BamHI-F (5′-CGGAGGATCCGTAGGACATGCGGAAACAAG-3′) and *fbaB*-SalI-R (5′-GTTACTGTCGACTTCCTTGTTATCAAA GTGG-3′). Expression of GST-tagged FbaB polypeptide and subsequent purification using glutathione sepharose affinity chromatography was conducted according to the manufacturer's protocol (GE Healthcare Munich).

Cloning of eukaryotic proteins and EC transfection

The PX domain of $p40^{PHOX}$ was cloned into pDsRed-Monomer-N1 and pTagRFP-N1, respectively, as described before (Catz *et al*., 2002) using human $p40^{PHOX}$ full-length cDNA template (imaGenes, Berlin, Germany). To construct CRIB-TagRFP, PCR was used to amplify the fragment encoding amino acids 60–141 of PAK1B using the primers: CRIB_EcoRI_fwd 5′-CGAATTCACACCATGGTACCTGGAGATAAAACAAAT-3′ and CRIB_SalI_rev 5′-CCGTCGACCATTTCTGGCTGTTGGATGTCT-3′, and pGEX-2T-PAK-CRIB as a template. The resulting fragment was gel purified and cloned in pTagRFP-N1 using EcoRI and SalI sites, yielding pCRIB-TagRFP. All constructs were sequenced before use. Plasmids were purified with the EndoFree plasmid purification kit (Qiagen, Hilden, Germany). HUVEC were then transfected with the Amaxa nucleofection system (AMAXA) applying the standard protocol as specified by the manufacturer. For ectopic expression of GTPase derivatives in HUVEC, wild-type Rac1 and the dominant-negative form of Rac1 (kindly provided by I. Just) were expressed in HUVEC as GFP-fusion proteins as previously described (Nerlich *et al*., 2009).

Quantification of FbaB surface localization by flow cytometry

Streptococcal strains were grown to mid-exponential phase in TSB medium and washed once in PBS. A total of 1×10^7 bacteria were suspended in 400 µl of PBS containing 0.5% FCS and incubated with 0.5 µg of anti-FbaB rabbit IgG for 30 min at 37°C. After washing in PBS the bacterial pellet was suspended in 100 µl of PBS containing a 1:300 dilution of an anti-rabbit ALEXA® Fluor 488 antibody and incubated for 30 min at 37°C. Bacteria were washed in PBS, fixed in PBS containing 3% para-formaldehyde and analysed by flow cytometry using a FACSCalibur (Becton Dickinson). Streptococci were detected using log-forward and log-side scatter dot plots, and a gating region was set to exclude debris and larger aggregates of bacteria. A total of 5×10^3 bacteria were analysed for fluorescence using log-scale amplification.

EC culture and invasion assay

Primary human large vascular cells isolated from umbilical cord (HUVEC) were purchased from PromoCell. EC were cultured and propagated in EGM-2 medium (PromoCell) according to the supplier's protocol in a cell incubator at 37°C and 5% CO_2. Cells were seeded on coverslips in multiwell plates (Nunc) and grown to 75% confluency. Streptococci were grown in TSB, harvested by centrifugation, washed and diluted in pre-warmed EGM-2 medium containing 5% FCS and used to infect EC with an moi of 25 for GBS strains and an moi of 50 for GAS WT strains as well as the FbaB Knock-out GAS strain. Infection was stopped after a maximum of 2 h of infection by washing the infected monolayer with EGM-2 medium and fixing with PBS containing 4% PFA. Distinct time points for fixation were used for monitoring early entry (60 min post infection) or subsequent trafficking (120 min post infection). For inhibition of lysosomal fusion events, the PI3 kinase inhibitor LY294002 was selected since class III PI3K is essential for endosomal fusion and subsequent trafficking into lysosomes. HUVEC were pre-incubated with 25 µM LY294002 for 45 min and infected.

Immunofluorescence and confocal microscopy

After fixation, infected EC monolayers were blocked for 30 min with PBS containing 10% FCS. Differential staining of streptococci was performed as previously described (Rohde *et al*., 2003). According to their respective label, intracellular bacteria appear red and extracellular yellow to green. F-actin, EEA1 and Lamp-1 were visualized as described (Kaur *et al*., 2010). In some experiments streptococci were labelled with secondary Cy5-conjugated antibodies. Following final washing, coverslips were mounted on glass slides using ProLong Gold anti-fade reagent (Molecular Probes). Mounted samples were examined using a confocal laser scanning microscope (LSM 510 Meta, Zeiss). Alternatively, images were recorded using a Zeiss inverted microscope 100 or a Zeiss Axiophot with an attached Zeiss Axiocam HRc digital camera and Zeiss Axiovision software 7.6. Images were processed for contrast and brightness using ImageJ (http://rsb.info.nih.gov/ij).

Determination of invasion rates and quantification of Lamp-1 association

Invasion rates of streptococcal strains or beads were determined by enumerating intracellular (red) bacteria or beads after infecting cells for 2 h with an initial moi of 25 for GBS strains, an moi of 50 for GAS strains, and in case of beads with an moi of 100. Invasion rates were expressed as either intracellular bacteria per 10 cells or % invasion. For Lamp-1 colocalization, the number of bacteria (red) residing within a Lamp-1-positive compartment was enumerated. A minimum of 100 cells were analysed per assay; assays were conducted in triplicate and repeated for at least three times on different days. Data represent means of one representative experiment conducted in triplicate.

Time-lapse microscopy

Live cell imaging was performed at 37°C in 5% CO_2 with cells expressing the GFP fusion of WT Rac1 as described elsewhere (Nerlich *et al*., 2009).

BSA-gold loading of HUVEC lysosomes

BSA-gold particles with a diameter of 15 nm were prepared by incubating 10 ml of the gold sole (pH 6.0) with 100 µg of BSA for 30 min at 20°C, followed by centrifugation at 20 000 r.p.m. in a TLD100 (Beckman) for 15 min, then a wash step with PBS. Lysosomes were pre-loaded by feeding HUVEC with BSA-gold 24 h prior to infection as described (Rohde *et al*., 2003). The following day, cells were infected and fixed after 120 min post infection and ultrathin sections analysed by transmission electron microscopy (TEM).

Transmission (TEM) and field emission scanning electron microscopy (FESEM)

For TEM analysis, HUVEC were grown in 6-cm-diameter culture dishes, infected, subsequently washed with EGM-2 medium, and fixed and embedded as described (von Kockritz-Blickwede *et al*., 2008). Images were recorded digitally with a Slow-Scan CCD-Camera (ProScan, 1024 × 1024) with ITEM-Software (Olympus

Soft Imaging Solutions). For FESEM analysis, HUVEC were grown and infected on coverslips, washed in EGM-2 medium and prepared as described (von Kockritz-Blickwede *et al.*, 2008). Brightness and contrast were adjusted with Adobe Photoshop CS3.

Whole-cell fibronectin-binding assay

Human fibronectin (Chemicon) was radiolabelled with ^{125}I via the Chloramine T method as described (Hunter and Greenwood, 1962). Streptococci were grown in TSB, washed in PBS containing 0.05% Tween (PBST) and suspended in PBST to give a final concentration of 1×10^8 bacteria per ml. Two hundred and fifty microlitres of the bacterial suspension was incubated with 20 ng of radiolabelled fibronectin (specific activity of 2.9 mCi mg^{-1}). After 1 h of incubation, unbound fibronectin was removed by washing bacteria with PBST and by measuring the amount of bound fibronectin in a gamma counter. Total counts of radiolabelled fibronectin in the assay were determined in parallel by TCA precipitation and formed the basis for the 100% value. Binding activity was expressed as the percentage of bound fibronectin compared with total fibronectin. Assays were performed in triplicate and experiments were repeated three times.

Latex bead internalization assay

Purified recombinant FbaB protein or GST in case was coupled to 3 μm latex beads (Sigma) and tested for coupling efficiency as described (Molinari *et al.*, 1997). HUVEC were seeded on coverslips as described above and co-incubated with FbaB or GST-coated latex beads with an moi of 100 for 1 h. Cells were then washed three times with EGM2 and fixed as described above. Double-immunofluorescent staining of intra- and extracellular beads was performed as described for streptococci except that rabbit anti-FbaB and anti-GST antibodies served as primary antibody. Intracellular (red) beads were enumerated by counting and internalization rates were expressed as % invasion. A minimum of 100 cells were analysed per assay; assays were conducted in triplicate and repeated for at least three times on different days. Data represent means of one representative experiment conducted in triplicate.

Statistical analyses

Statistical comparisons were made using the Student's paired *t*-test with Graph Pad Prism software. Values are expressed as means ± SD.

Acknowledgements

We thank N. Janze and I. Schleicher for excellent technical assistance and I. Just for providing the Rac1 constructs. S.R.T. gratefully acknowledges funding through the 'Reentry Program' given by the Helmholtz Association, Germany, and funding through the 'CAREPNEUMO' programme given by the EU Commission (contract No. 223111). A.N. gratefully acknowledges funding through the 'ASSIST' programme given by the EU Commission (contract No. 032390). J.N.C. was supported by a National Health and Medical Research Council of Australia grant (514639).

References

Bessen, D.E., and Kalia, A. (2002) Genomic localization of a T serotype locus to a recombinatorial zone encoding extracellular matrix-binding proteins in *Streptococcus pyogenes*. *Infect Immun* **70:** 1159–1167.

Catz, S.D., Johnson, J.L., and Babior, B.M. (2002) The C2A domain of JFC1 binds to 3′-phosphorylated phosphoinositides and directs plasma membrane association in living cells. *Proc Natl Acad Sci USA* **99:** 11652–11657.

Cunningham, M.W. (2000) Pathogenesis of group A streptococcal infections. *Clin Microbiol Rev* **13:** 470–511.

Delvecchio, A., Currie, B.J., McArthur, J.D., Walker, M.J., and Sriprakash, K.S. (2002) *Streptococcus pyogenes* prtFII, but not sfbI, sfbII or fbp54, is represented more frequently among invasive-disease isolates of tropical Australia. *Epidemiol Infect* **128:** 391–396.

Dinkla, K., Rohde, M., Jansen, W.T., Kaplan, E.L., Chhatwal, G.S., and Talay, S.R. (2003) Rheumatic fever-associated *Streptococcus pyogenes* isolates aggregate collagen. *J Clin Invest* **111:** 1905–1912.

Dombek, P.E., Cue, D., Sedgewick, J., Lam, H., Ruschkowski, S., Finlay, B.B., and Cleary, P.P. (1999) High-frequency intracellular invasion of epithelial cells by serotype M1 group A streptococci: M1 protein-mediated invasion and cytoskeletal rearrangements. *Mol Microbiol* **31:** 859–870.

Ellson, C.D., Gobert-Gosse, S., Anderson, K.E., Davidson, K., Erdjument-Bromage, H., Tempst, P., *et al.* (2001) PtdIns(3)P regulates the neutrophil oxidase complex by binding to the PX domain of p40(phox). *Nat Cell Biol* **3:** 679–682.

Haas, A. (2007) The phagosome: compartment with a license to kill. *Traffic* **8:** 311–330.

Hagan, R.M., Björnsson, R., McMahon, S.A., Schomburg, B., Braithwaite, V., Bühl, M., *et al.* (2010) NMR spectroscopic and theoretical analysis of a spontaneously formed Lys–Asp isopeptide bond. *Angew Chem Int Ed Engl* **49:** 8421–8425.

Hunter, W.J., and Greenwood, F.C. (1962) Preparation of iodine 131 labeled human growth hormone of high specific activity. *Nature* **194:** 495–496.

Inagaki, Y., Myouga, F., Kawabata, H., Yamai, S., and Watanabe, H. (2000) Genomic differences in *Streptococcus pyogenes* serotype M3 between recent isolates associated with toxic shock-like syndrome and past clinical isolates. *J Infect Dis* **181:** 975–983.

Itoh, R.E., Kurokawa, K., Ohba, Y., Yoshizaki, H., Mochizuki, N., and Matsuda, M. (2002) Activation of rac and cdc42 video imaged by fluorescent resonance energy transfer-based single-molecule probes in the membrane of living cells. *Mol Cell Biol* **22:** 6582–6591.

Jaffe, J., Natanson-Yaron, S., Caparon, M.G., and Hanski, E. (1996) Protein F2, a novel fibronectin-binding protein from *Streptococcus pyogenes*, possesses two binding domains. *Mol Microbiol* **21:** 373–384.

Kaur, S.J., Nerlich, A., Bergmann, S., Rohde, M., Fulde, M., Zahner, D., *et al.* (2010) The CXC chemokine-degrading protease SpyCep of *Streptococcus pyogenes* promotes its uptake into endothelial cells. *J Biol Chem* **285:** 27798–27805.

von Kockritz-Blickwede, M., Goldmann, O., Thulin, P., Heinemann, K., Norrby-Teglund, A., Rohde, M., and Medina, E.

(2008) Phagocytosis-independent antimicrobial activity of mast cells by means of extracellular trap formation. *Blood* **111:** 3070–3080.

Molinari, G., Talay, S.R., Valentin-Weigand, P., Rohde, M., and Chhatwal, G.S. (1997) The fibronectin-binding protein of *Streptococcus pyogenes*, SfbI, is involved in the internalization of group A streptococci by epithelial cells. *Infect Immun* **65:** 1357–1363.

Mora, M., Bensi, G., Capo, S., Falugi, F., Zingaretti, C., Manetti, A.G., *et al.* (2005) Group A *Streptococcus* produce pilus-like structures containing protective antigens and Lancefield T antigens. *Proc Natl Acad Sci USA* **102:** 15641–15646.

Neeman, R., Keller, N., Barzilai, A., Korenman, Z., and Sela, S. (1998) Prevalence of internalisation-associated gene, *prtF1*, among persisting group-A streptococcus strains isolated from asymptomatic carriers. *Lancet* **352:** 1974–1977.

Nerlich, A., Rohde, M., Talay, S.R., Genth, H., Just, I., and Chhatwal, G.S. (2009) Invasion of endothelial cells by tissue-invasive M3 type group A streptococci requires Src kinase and activation of Rac1 by a phosphatidylinositol 3-kinase-independent mechanism. *J Biol Chem* **284:** 20319–20328.

Ramachandran, V., McArthur, J.D., Behm, C.E., Gutzeit, C., Dowton, M., Fagan, P.K., *et al.* (2004) Two distinct genotypes of prtF2, encoding a fibronectin binding protein, and evolution of the gene family in *Streptococcus pyogenes*. *J Bacteriol* **186:** 7601–7609.

Rocha, C.L., and Fischetti, V.A. (1999) Identification and characterization of a novel fibronectin-binding protein on the surface of group A streptococci. *Infect Immun* **67:** 2720–2728.

Rohde, M., Muller, E., Chhatwal, G.S., and Talay, S.R. (2003) Host cell caveolae act as an entry-port for group A streptococci. *Cell Microbiol* **5:** 323–342.

Rohde, M., Graham, R.M., Branitzki-Heinemann, K., Borchers, P., Preuss, C., Schleicher, I., *et al.* (2011) Differences in the aromatic domain of homologous streptococcal fibronectin-binding proteins trigger different cell invasion mechanisms and survival rates. *Cell Microbiol* **13:** 450–468.

Schwarz-Linek, U., Werner, J.M., Pickford, A.R., Gurusiddappa, S., Kim, J.H., Pilka, E.S., *et al.* (2003) Pathogenic bacteria attach to human fibronectin through a tandem beta-zipper. *Nature* **423:** 177–181.

Schwarz-Linek, U., Hook, M., and Potts, J.R. (2006) Fibronectin-binding proteins of gram-positive cocci. *Microbes Infect* **8:** 2291–2298.

Stevens, D.L. (2000) Streptococcal toxic shock syndrome associated with necrotizing fasciitis. *Annu Rev Med* **51:** 271–288.

Stevens, D.L., Tanner, M.H., Winship, J., Swarts, R., Ries, K.M., Schlievert, P.M., and Kaplan, E. (1989) Severe group A streptococcal infections associated with a toxic shock-like syndrome and scarlet fever toxin A. *N Engl J Med* **321:** 1–7.

Talay, S.R. (2005) Gram-positive adhesins. *Contrib Microbiol* **12:** 90–113.

Talay, S.R., Zock, A., Rohde, M., Molinari, G., Oggioni, M., Pozzi, G., *et al.* (2000) Co-operative binding of human fibronectin to Sfbl protein triggers streptococcal invasion into respiratory epithelial cells. *Cell Microbiol* **2:** 521–535.

Telford, J.L., Barocchi, M.A., Margarit, I., Rappuoli, R., and Grandi, G. (2006) Pili in gram-positive pathogens. *Nat Rev Microbiol* **4:** 509–519.

Terao, Y., Kawabata, S., Nakata, M., Nakagawa, I., and Hamada, S. (2002) Molecular characterization of a novel fibronectin-binding protein of *Streptococcus pyogenes* strains isolated from toxic shock-like syndrome patients. *J Biol Chem* **277:** 47428–47435.

Vieira, O.V., Botelho, R.J., Rameh, L., Brachmann, S.M., Matsuo, T., Davidson, H.W., *et al.* (2001) Distinct roles of class I and class III phosphatidylinositol 3-kinases in phagosome formation and maturation. *J Cell Biol* **155:** 19–25.

Zinkernagel, A.S., Timmer, A.M., Pence, M.A., Locke, J.B., Buchanan, J.T., Turner, C.E., *et al.* (2008) The IL-8 protease SpyCEP/ScpC of group A *Streptococcus* promotes resistance to neutrophil killing. *Cell Host Microbe* **4:** 170–178.

Supporting information

Additional Supporting Information may be found in the online version of this article:

Fig. S1. GBS WT infection of HUVEC and phase-contrast images demonstrating HUVEC monolayer integrity.

A. Phase-contrast images underlying the fluorescent image of Fig. 1C, showing GBS-FbaB-infected HUVEC. Bar represents 5 μm.

B. Phase-contrast image underlying the fluorescent images of Fig. 1H, showing FbaB-coated latex beads on and in HUVEC. Bar represents 1 μm.

C. Double immunofluorescent image (left panel) and phase-contrast image (middle panel) of the same section showing extracellular (yellow) WT GBS on confluent HUVEC after 2 h of infection. WT GBS are not invasive and thus, no intracellular (red) bacteria were detected. A scanning electron micrograph (right panel) shows WT GBS attaching to the glass coverslip on a semi-confluent HUVEC monolayer after 2 h of infection. Bars represent 10 μm.

Fig. S2. Quantification of HEp-2 cell invasion and phase-contrast images demonstrating cell layer integrity.

A–D. Phase-contrast images underlying the fluorescent images of Fig. 4, showing GBS-FbaB and M3 GAS-infected HUVEC and HEp-2 cells. Bars represent 15 μm.

E. Quantification of HEp-2 cell invasion. Epithelial layers were simultaneously infected with an SfbI-expressing M12 GAS isolate, the M3 GAS strain, as well as the GBS-FbaB strain. Invasion rates were determined after 2 h of infection by counting intracellular (red) bacteria per cell. The graph shows mean numbers (± SD) of intracellular bacteria per 10 cells from three independent experiments.

F. Double immunofluorescent and phase-contrast image of HEp-2 cells infected with M12 GAS. Note that in the phase-contrast image bacteria are not in focus, due to the thickness of HEp-2 cells. Bars represent 15 μm.

Movie S1. Time-lapse microscopy of Rac1 accumulation along a HUVEC-invading FbaB-expressing streptococcal chain.

Please note: Wiley-Blackwell are not responsible for the content or functionality of any supporting materials supplied by the authors. Any queries (other than missing material) should be directed to the corresponding author for the article.